## Appendix for

# STIC2 selectively binds ribosome-nascent chain complexes in the cotranslational sorting of *Arabidopsis* thylakoid proteins

**Stolle, Osterhoff et al.**

**Content:**

## Appendix Figures

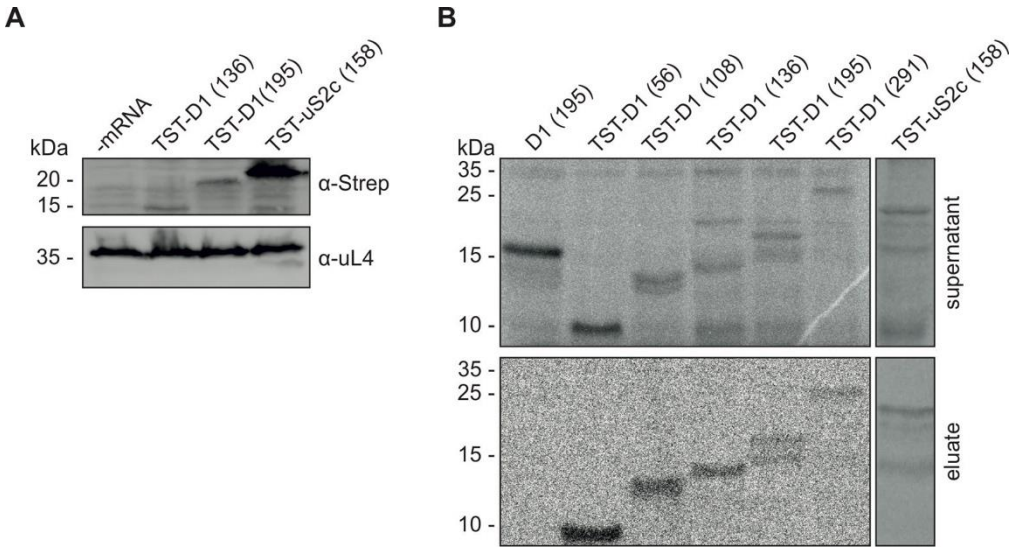


**Appendix Figure S1** Sucrose gradient enrichment and affinity purification of ribosomes translating TST-tagged peptides

Stalled RNCs with nascent TST-D1 peptides of the indicated lengths and TST-uS2c (158) were generated using the pea chloroplast-derived *in vitro* translation system. Details on the various constructs are given in Figure 1.

**A**. Enrichment of TST-D1 (136), TST-D1 (195), and TST-uS2c (158) RNCs via 1 M sucrose cushion centrifugation. A translation sample lacking mRNA was used as a control. The sedimented protein complexes were separated with SDS-PAGE and applied to Western blot analysis. RNCs with 15 kDa and 20 kDa TST-D1 or 22 kDa TST-uS2c peptides were detected with antibody against the TST (α-Strep) and the ribosomal protein uL4 (α-uL4).

**B**. In the presence of radiolabeled methionine, truncated D1 and uS2c peptides were synthesized *in vitro* and subsequently incubated with MagStrep XT magnetic beads for affinity-based purification. A truncated D1 (195) peptide lacking the TST was synthesized as a negative control for the affinity purification (first lane). Unbound RNCs were removed with the supernatant in a magnetic separator. The magnetic beads were washed and remaining RNCs were subsequently released with native elution. Supernatant (upper panel) and eluate (lower panel) were subjected to SDS-PAGE and synthesized peptides were detected by phosphor imaging.

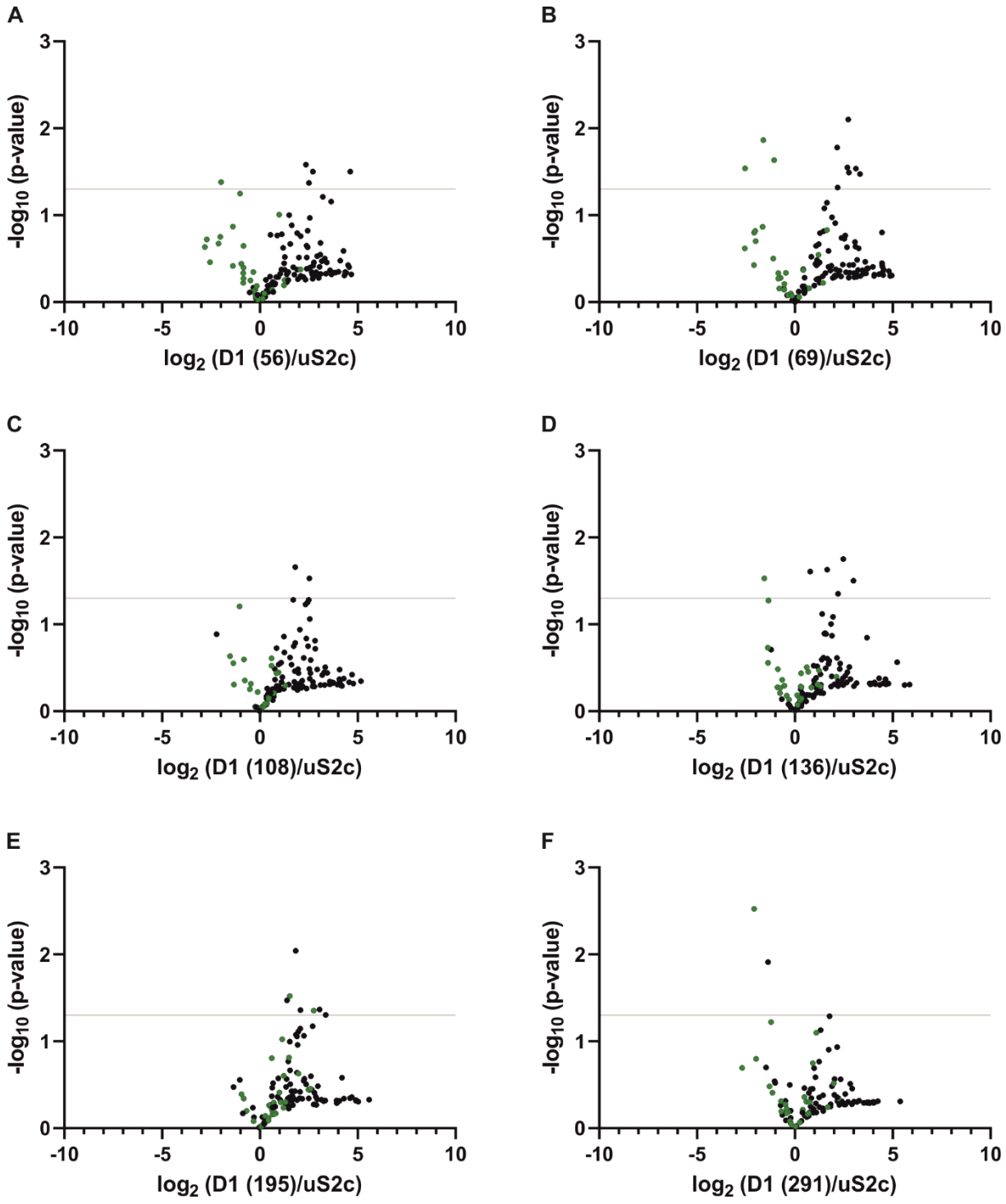


**Appendix Figure S2** Comparison of proteins identified in TST-D1 and TST-uS2c RNCs

**A**-**F**. Volcano plots representing proteins identified by tandem MS in RNCs with TST-uS2c (158) and TST-D1 peptides of different length. *P*-values ($-\log_{10}$) were plotted against the ratio of label-free quantification intensity means ($\log_2$). The *p*-values were determined by two-sided *t*-test ($p \leq 0.05$). Ribosomal proteins are labeled in green.

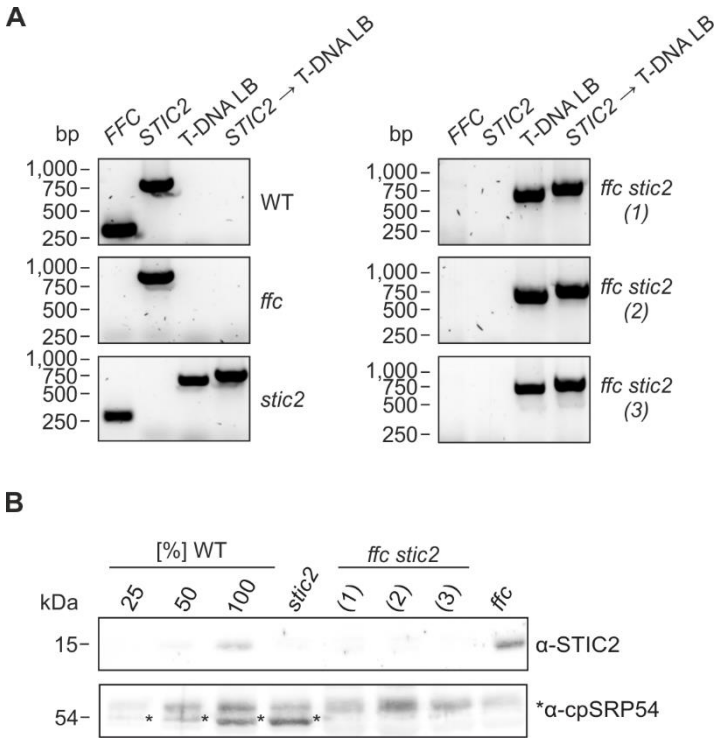


**Appendix Figure S3** Verification of homozygous *ffc stic2* plants

The *Arabidopsis thaliana* double mutant *ffc1-2 stic2-3* (*ffc stic2*) was created by crossing the homozygous single mutant plants *ffc1-2* (*ffc*) and *stic2-3* (*stic2*) with *stic2* as female plant. Putative *ffc stic2* double mutants (*ffc stic2* (1), (2), and (3)) of the F2 generation were verified via genotyping PCRs (**A**) and immunoblotting (**B**).

**A.** Wild-type plants of the ecotype Columbia-0 (Col-0), the *ffc* and *stic2* mutants were used as controls. Gene-specific primer combinations were used to prove DNA insertions in ffc (At5g03940, lane FFC) and stic2 (At2g24020, lane STIC2). The T-DNA insertion was verified by amplifying its left border (T-DNA LB). Proof of proper T-DNA insertion in stic2 was analyzed by amplification of the junction from the 5'UTR to the T-DNA left border. Bands at 319, 821, about 600 and 750 bp display PCR products of ffc, stic2, the T-DNA left border and the junction from stic2 5' UTR to the T-DNA left border.

**B.** Total protein extracts from leaves of 5-week-old *Arabidopsis thaliana* plants (wild-type (Col-0), *stic2, ffc* and the putative double mutants *ffc stic2 (1), (2) and (3)* were separated by SDS-PAGE and analyzed via immunoblotting regarding the expression of cpSRP54 and STIC2. The loading control is the same as in Figure 3.

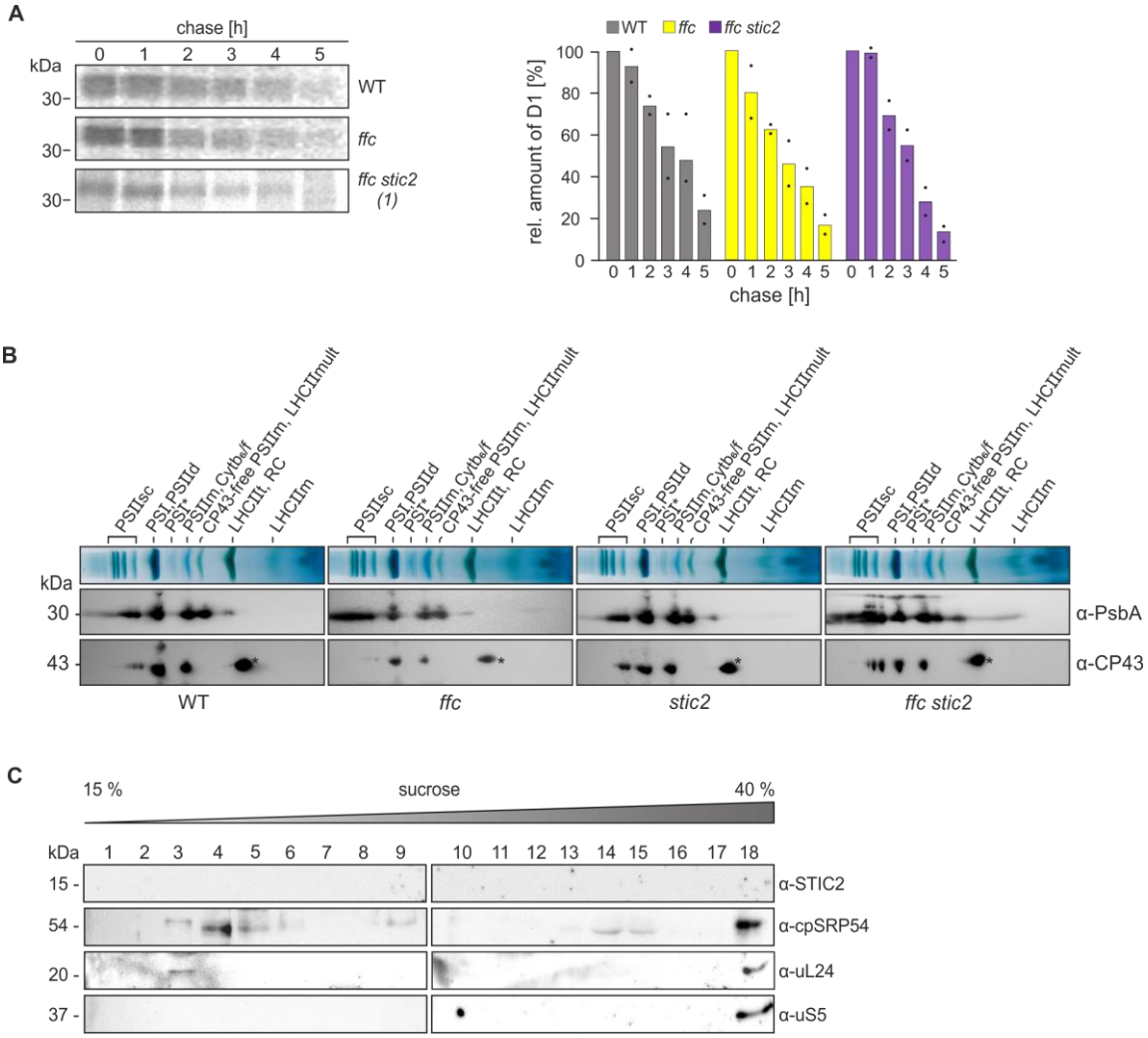


**Appendix Figure S4** Characterization of *Arabidopsis* WT and mutant plants

**A.** Leaf discs of wild type (Col-0) and the indicated *A. thaliana* mutants were labeled with [$^{35}$S]-methionine in presence of cycloheximide for 60 min in ambient light (0 h chase). After removal of [$^{35}$S]-methionine the labeled D1 protein was chased for 1, 2, 3, 4 and 5 hours under high light (1000 µmol photons $m^{-2}$ $s^{-1}$). Labeled thylakoid membrane proteins were used for SDS-PAGE and phosphor imaging. Signals from two independent experiments were quantified in relation to 0 h chase time using ImageJ.

**B.** Thylakoids isolated from chloroplasts of *Arabidopsis thaliana* plants (Col-0, *ffc1-2* (*ffc*), *stic2-3* (*stic2*) and *ffc1-2 stic2-3* (*ffc stic2*)) were solubilized in DDM and separated by BN-PAGE based on equal chlorophyll loading (10 µg chlorophyll/lane). The identification of detected bands was accomplished in accordance with published BN-PAGE profiles of Arabidopsis thylakoids (Granvogl et al. 2006; Armbruster et al. 2010; Wittenberg et al. 2017; Che et al. 2022). Photosystem I and II (PSI and II), PSII supercomplexes ($PSII_{sc}$), PSII dimers ($PSII_d$), PSI assembly intermediate (PSI*), monomeric PSII ($PSII_m$) and Cytochrom $b_6$/f complex ($Cytb_6$/f), CP43-free PSII monomers (CP43-free $PSII_m$) and multimeric light harvesting antenna complex II ($LHCII_{mult}$), trimeric LHCII ($LHCII_t$), reaction center-like complex (RC), monomeric ($LHCII_m$). Additionally, the protein complex subunit composition was determined by two-dimensional BN-PAGE/SDS-PAGE analysis followed by immunoblot analysis using α-PsbA and α-CP43 antibodies (Agrisera) directed against the PS II subunits D1 and CP43, respectively. The asterisk (*) marks free CP43 protein.

**C.** A cell extract of the *stic2-3* plant was subjected to sucrose gradient centrifugation in the presence of chloramphenicol. Gradient fractions were separated by SDS-PAGE and applied to immunoblotting using the indicated antibodies.

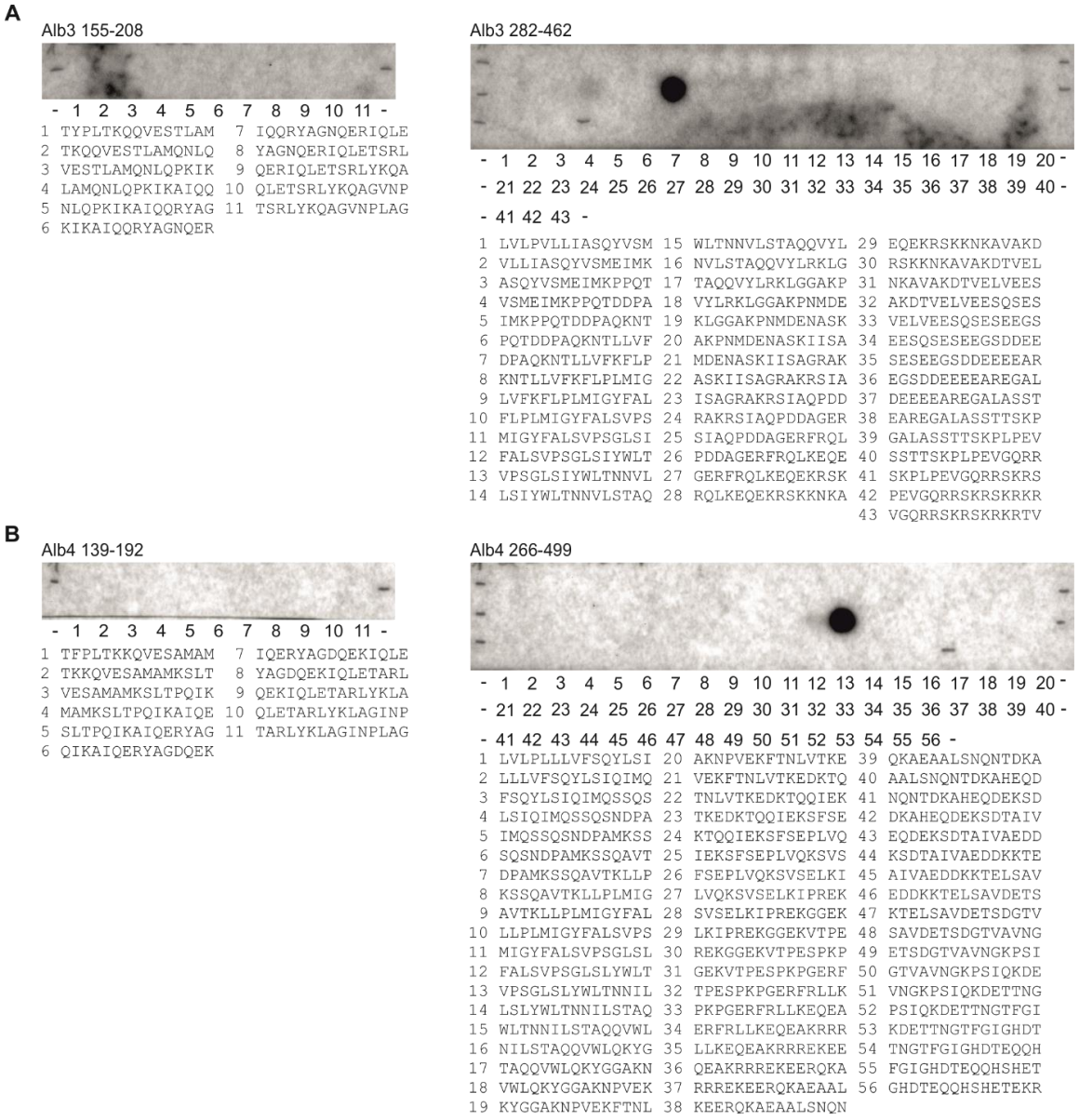


**Appendix Figure S5** Membrane bound Alb3- and Alb4-peptide arrays used for the interaction analyses with STIC2

**A**. Peptides covering Alb3 residues 155-208 and 282-462 (15mer peptides) were incubated with His-mSTIC2 (aa 49-182) at a final concentration of 5 µg/ml. The peptide sequences are indicated below the pepspot membranes. An antibody-HRP conjugate against the His-tag was used to detect His-mSTIC2 protein on pepspot membranes.

**B**. Peptides covering Alb4 residues 139-192 and 266-499 were analyzed as in **A**.

Further details are given in Materials and Methods and Figure 5A in the main text. The peptide arrays shown in the right panels of this figure and in Figure 5A are identical.

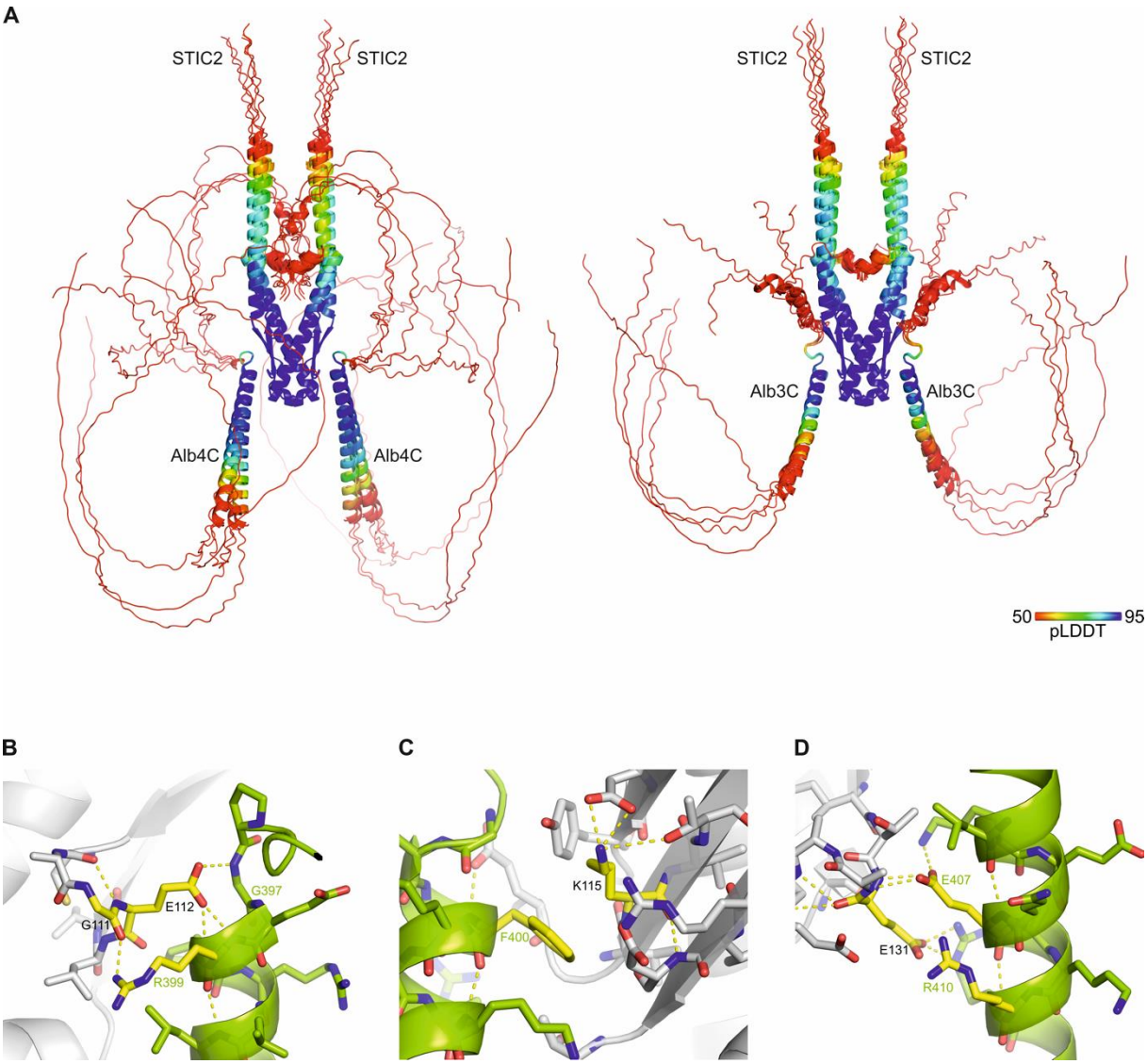


**Appendix Figure S6** The binding interface of STIC2 with Alb4C and Alb3C

**A**. Alphafold-Multimer models of STIC2 in complex with Alb4C (left) and Alb3C (right). The five models of each prediction run are superposed in cartoon representation. Coloring according to the residue specific pLDDT quality score from 50-95 (see inset), blue being the most reliable.

**B-D**. Interactions between STIC2 and Alb4C. Detailed view of interactions of residues discussed in the text. Proteins are shown in cartoon representation in grey and green for STIC2 and Alb4C, respectively. Residues under investigation are shown as yellow sticks with their polar interactions as defined in Pymol. In addition, residues within 4 Å are shown as grey/green sticks.

## Appendix Tables

### Appendix Table S1 Primer

| Construct | Sequence (5' → 3') | Cloning strategy |
|---|---|---|
| **Generation of DNA templates for *in vitro* transcription** | | |
| TST-D1 (aa 1-56) | for: GTAATACGACTCACTATAGGGCGAGTAACAAGC CCTTAATTCTATAGTTA<br>rev: AGGGGCAGCAATGAAAGCG | |
| TST-D1 (aa 1-69) | for: GTAATACGACTCACTATAGGGCGAGTAACAAGC CCTTAATTCTATAGTTA<br>rev: TCCAGAAACAGGCTCACGAATACC | |
| TST-D1 (aa 1-108) | for: GTAATACGACTCACTATAGGGCGAGTAACAAGC CCTTAATTCTATAGTTA<br>rev: CGTTGTATAACCATTCATCAACGGATGC | |
| TST-D1 (aa 1-136) | for: GTAATACGACTCACTATAGGGCGAGTAACAAGC CCTTAATTCTATAGTTA<br>rev: GACGAAAACTAAGTTCCCACTCACG | |
| TST-D1 (aa 1-195) | for: GTAATACGACTCACTATAGGGCGAGTAACAAGC CCTTAATTCTATAGTTA<br>rev: GGTGCATAAGAATATTATGCTCAGCC | |
| TST-D1 (aa 1-291) | for: GTAATACGACTCACTATAGGGCGAGTAACAAGC CCTTAATTCTATAGTTA<br>rev: GCTGATACCTAACGCGGTAAACCAG | |
| TST-uS2c (aa 1-58) | for: TAATACGACTCACTATAGGG<br>rev: CATATATTTAATCCCGCCTAGATATG | |
| **Genotyping PCRs** | | |
| *FFC* | for: GATAAAGGCATGATGGACGAATTAAAAGACG<br>rev: CAAACCTCCTTGACACTCAAAGCAGCACCACC | |
| *STIC2* | for: CAATCTAAGCTCAAAAAAAGAGTTAAAGTGACG<br>rev: GAACACGTACAGCTTCCACTTGAACAACC | |
| T-DNA LB | for: CTGCCTGTATCGAGTGGTGA<br>rev: ACTTAATCGCCTTGCAGCAC | |
| *STIC2* → T-DNA LB | for: CAATCTAAGCTCAAAAAAAGAGTTAAAGTGACG<br>rev: ACTTAATCGCCTTGCAGCAC | |
| **pET-Duet1-** | | |
| STIC2 (aa 49-182) | for: CATCACCATCATCACCACAGCCAGGTGAATGGA TTATTTGGAGGTGGAA<br>rev: GCGGCCGCAAGCTTGTCGACTTACTTCATTCC TTCGCTGA | InFusion |
| STIC2 (aa 64-182) | for: TCATCACCACAGCCAGGATCCGGATGGACAAT CAAAGGCAGGA<br>rev: GCGGCCGCAAGCTTGTCGACTTACTTCATTCC TTCGCTGA | InFusion |
| STIC2 G111L | for: GATGGTTATTGTGCATTAGAGCTTGTCAAGGTT AC<br>rev: GTAACCTTGACAAGCTCTAATGCACAATAACCA TC | QuikChange mutagenesis |

| | | |
|---|---|---|
| STIC2 E112A | for: GGTTATTGTGCAGGCGCGCTTGTCAAGGTTAC G<br>rev: CGTAACCTTGACAAGCGCGCCTGCACAATAACC | QuikChange mutagenesis |
| STIC2 K115A | for: GCAGGCGAGCTTGTCGCGGTTACGTTATCAGG<br>rev: CCTGATAACGTAACCGCGACAAGCTCGCCTGC | QuikChange mutagenesis |
| STIC2 E131G | for: [5' phos] GGAGCAGCAATGGAACTAGGTTCC<br>rev: [5' phos] GGTAATATCAGTACGGATTGG | Site-directed mutagenesis |
| **pET29b-** | | |
| Alb3CΔIII (aa 350-462 Δ386-403) | for: GGATGATGCGGCGGTGGCGAAAGATACCGT<br>rev: TCGCCACCGCCGCATCATCCGGCTGCGC | InFusion |
| Alb4CΔIII (aa 334-499 Δ397-414) | for: GAATGCCCCAAACCTGAAGAGAGGCAGAAAGC TGAAGCAG<br>rev: TTTCTGCCTCTCTTCAGGTTTGGGGCATTCTG GGGTCACC | InFusion |
| Alb4C R399G | for: [5'phos] GGGTTTAGGCTGCTGAAAGAGCAA<br>rev: [5'phos] TTCACCAGGTTTGGGGCATTC | Site-directed mutagenesis |
| Alb4C F400G | for: [5'phos] GGTAGGCTGCTGAAAGAGCAAGAA<br>rev: [5'phos] CCTTTCACCAGGTTTGGGGCA | Site-directed mutagenesis |
| Alb4C E407G | for: [5'phos] GGAGCAAAGAGACGTCGAGAAAAA<br>rev: [5'phos] TTGCTCTTTCAGCAGCCTAAA | Site-directed mutagenesis |
| Alb4C R410G | for: [5'phos] GGACGTCGAGAAAAAGAAGAGAGG<br>rev: [5'phos] CTTTGCTTCTTGCTCTTTCAGCAG | Site-directed mutagenesis |
| **pGEX4T3-** | | |
| STIC2 (aa 49-182) | for: ATCTGGTTCCGCGTGGATCCGTGAATGGATTAT TTGG<br>rev: GGCCGCTCGAGTCGACTTACTTCATTCCTTCG CTGA | InFusion |
| STIC2 G111L | for: ATCTGGTTCCGCGTGGATCCGTGAATGGATTAT TTGG<br>rev: GGCCGCTCGAGTCGACTTACTTCATTCCTTCG CTGA | Classical cloning |
| STIC2 E112A | for: ATCTGGTTCCGCGTGGATCCGTGAATGGATTAT TTGG<br>rev: GGCCGCTCGAGTCGACTTACTTCATTCCTTCG CTGA | Classical cloning |
| STIC2 K115A | for: ATCTGGTTCCGCGTGGATCCGTGAATGGATTAT TTGG<br>rev: GGCCGCTCGAGTCGACTTACTTCATTCCTTCG CTGA | Classical cloning |
| STIC2 E112A K115A | for: [5'phos]GCGCTTGTCGCGGTTACGTTATCA<br>rev: [5'phos]GCCTGCACAATAACCATCAAATTC | Site-directed mutagenesis |
| STIC2 E131G | for: AGTGGATCCGATGGACAATCAAAGGCAGGA<br>rev: GGCCGCTCGAGTCGACTTACTTCATTCCTTCG CTGA | Classical cloning |

**Appendix Supplementary Materials and Methods**

*Sucrose gradient enrichment of RNCs*

For sucrose cushion centrifugation 160 µl of the translation reaction were loaded on a 2.9 ml sucrose cushion (1 M sucrose, 30 mM HEPES pH 7.7, 9 mM magnesium acetate, 70 mM potassium acetate, 2 µg/ml antipain, 2 µg/ml leupeptin, 5 mM DTT, 0.25 mg/ml chloramphenicol, 0.1 mM AEBSF) and centrifuged (270,000 g, 90 min, 4°C, TLA 100.3, Beckman Coulter). The pellet was solubilized in sample buffer and subsequently applied to SDS-PAGE and Western blot analyses.

*Affinity purification $^{35}$S-methionine labelled RNCs*

For SDS-PAGE and subsequent autoradiography analyses, the 40 µl *in vitro* translation reactions contained 20 µM 19 amino acid mix (Promega) and 0.45 µCi/µl of [$^{35}$S]-methionine (>1,000 Ci/mmol, Hartmann Analytics). The isolation of RNCs with MagStrep XT magnetic beads was essentially performed as described above with 30 µl of bead suspension.

*Genomic DNA extraction and genotyping of Arabidopsis thaliana ffc stic2 double mutants*

Potential *ffc stic2* double mutants were genotyped via PCR. Genomic DNA serving as template DNA was extracted according to Edwards et al. (1991) with the following modifications. After extraction of DNA from 2-3 small leaves, the air-dried DNA pellet was resuspended in 40 µl 10 mM Tris pH 6.7, 0.1 mM EDTA. Dissolved DNA is then incubated at 55°C for 15 min and briefly vortexed every 5 min. Subsequently, unresolved DNA and impurities were sedimented (5 min, 14,000 rpm, RT). The DNA-containing supernatant was further used for genotyping PCRs using GoTaq® Polymerase (Promega). The 10 kb DNA insertion into intron 8 in At5g03940 (*ffc*) was analyzed using a primer combination binding in exon 8 and 9 (Appendix Table S2). Primer binding in the 5' UTR of At2g24020 (*stic2*) and its coding sequence were used to analyze the T-DNA insertion into At2g24020. T-DNA insertion was verified by amplifying the T-DNA's left border and its localization within the 5' UTR of stic2 was verified by amplification of the transition from the stic2 5' UTR to the T-DNA.

*Blue-native-polyacrylamide gel electrophoresis*

Thylakoids isolated from chloroplasts of from *Arabidopsis thaliana* plants (Col-0, *ffc1-2* (*ffc*), *stic2-3* (*stic2*) and *ffc1-2 stic2-3* (*ffc stic2*)) were solubilized with 1.5% (w/v) n-dodecyl-β-D-maltosid (DDM) at a chlorophyll concentration of 1 mg/mL. The multiprotein complexes were separated by a 4-16% Blue-native-polyacrylamide gel electrophoresis (BN-PAGE) gradient according to the manufacturer's instructions (Invitrogen) using total amounts of 10 µg chlorophyll/lane.

**Appendix Supplementary References**

Armbruster U, Zühlke J, Rengstl B, Kreller R, Makarenko E, Rühle T, Schünemann D, Jahns P, Weisshaar B, Nickelsen J et al. (2010) The Arabidopsis thylakoid protein PAM68 is required for efficient D1 biogenesis and photosystem II assembly. *Plant Cell* 22: 3439–3460. DOI: 10.1105/tpc.110.077453.

Che L, Meng H, Ruan J, Peng L, Zhang L (2022) Rubredoxin 1 Is Required for Formation of the Functional Photosystem II Core Complex in Arabidopsis thaliana. *Front Plant Sci* 13: 824358. DOI: 10.3389/fpls.2022.824358.

Edwards K, Johnstone C, Thompson C (1991) A simple and rapid method for the preparation of plant genomic DNA for PCR analysis. *Nucleic Acids Res* 19: 1349. DOI: 10.1093/nar/19.6.1349

Granvogl B, Reisinger V, Eichacker LA (2006) Mapping the proteome of thylakoid membranes by de novo sequencing of intermembrane peptide domains. *Proteomics* 6: 3681–3695. DOI: 10.1002/pmic.200500924.

Wittenberg G, Järvi S, Hojka M, Tóth SZ, Meyer EH, Aro EM, Schöttler MA, Bock R (2017) Identification and characterization of a stable intermediate in photosystem I assembly in tobacco. *Plant J* 90: 478–490. DOI: 10.1111/tpj.13505